Pergamon

PII: S0306-4522(97)00380-1

Neuroscience Vol. 83, No. 1, pp. 15–25, 1998

0306–4522/98 $19.00+0.00

MODIFICATION OF DISCHARGE PATTERNS OF NEOCORTICAL NEURONS BY INDUCED OSCILLATIONS OF THE MEMBRANE POTENTIAL

M. VOLGUSHEV,*†‡§ M. CHISTIAKOVA*†‡ and W. SINGER*

*Max Planck Institute for Brain Research, Deutschordenstrasse 46, D-60528 Frankfurt/Main, Germany

†Institute of Higher Nervous Activity and Neurophysiology, Russian Academy of Sciences, Butlerova 5a, 117485 Moscow, Russia

‡Ruhr-Universität Bochum, Department of Neurophysiology, MA 4/149, D-44780 Bochum, Germany

Abstract—We investigated, with whole-cell recordings from rat visual cortex slices, how sinusoidal modulation of the membrane potential affects signal transmission. Subthreshold oscillations activate tetrodotoxin sensitive, transient inward currents whose threshold, phase lag and duration change with modulation frequency. These periodically recurring phases of enhanced excitability affect synaptic transmission in two ways. Weak and short lasting excitatory postsynaptic potentials evoke discharges only if they are coincident within a few milliseconds with these active membrane responses. Long-lasting, *N*-methyl-D-aspartate-mediated or polysynaptic excitatory postsynaptic potentials, by contrast, evoke trains of spikes, that are precisely time-locked to the oscillations and may last for more than 100 ms.

Thus, oscillations impose a precise temporal window for the integration of synaptic inputs, favouring coincidence detection and they generate temporally-structured responses whose timing and amplitude are largely independent of the input. These properties are ideally suited for the synchronization of neuronal activity and the encoding of information in the precise timing of discharges.

A preliminary account of these data has appeared in an abstract form [Volgushev M. *et al.* (1995) *Eur. J. Neurosci.* **8**, 77]. © 1997 IBRO. Published by Elsevier Science Ltd.

Key words: visual cortex, oscillations, synchronization, temporal coding, slices, rat.

Both cortical and subcortical neuronal networks tend to engage in oscillatory activity that covers a wide range of frequencies (for review see Refs 37, 42). A fraction of central neurons are endowed with pacemaker currents that favour the generation of rhythmic activity.[1,9,10,16,18,21,22,35] Rhythmic activity is also generated by network interactions between excitatory and inhibitory neurons and recent evidence indicates that inhibitory neurons play an important role not only in oscillatory patterning but also in the synchronization of neuronal discharges, both in the neocortex and in the hippocampus.[3–5,17,25,44,48,49] Thus oscillations can result from pacemaker mechanisms in individual cells or from reciprocal interactions among coupled neurons and typically, both mechanisms act in combination.[23,24] Pacemakers stabilize rhythmic activity and network interactions entrain neurons into oscillatory firing patterns. Experimental evidence suggests that an oscillatory patterning of neuronal activity may be instrumental for the synchronization of the discharges of spatially-distributed neurons.[19] Synchronization, in turn, raises with high temporal precision the saliency of discharges that have become synchronous[2,24] and this can be exploited to select with high temporal precision subsets of neuronal responses for further processing. It has been proposed, therefore, that synchronization of neuronal responses is used to dynamically associate selected subsets of active neurons into functionally coherent assemblies and to thereby accomplish binding functions that need to be achieved in parallel distributed processing.[36,47] Moreover, it is likely that precise synchronization of neuronal activity is important for use-dependent synaptic modifications such as long-term potentiation and long-term depression because both the occurrence and the polarity of the modifications depend critically on the relative timing of pre- and postsynaptic activation and hence on coincidence detection.[12–14,27,28]

Because of the putative significance of synchrony in neuronal processing and the role of oscillatory patterning in the establishment of synchrony, we examined how an oscillatory modulation of the membrane potential influences spike generation and

§To whom correspondence should be addressed.

Abbreviations: AMPA, α-amino-3-hydroxy-5-methylisoxazole-4-propionate; EGTA, ethyleneglycolbis(aminoethylether) tetra-acetate; EPSC, excitatory postsynaptic current; EPSP, excitatory postsynaptic potential; HEPES, N-2-hydroxyethylpiperazine-N′-2-ethanesulphonic acid; NMDA, *N*-methyl-D-aspartate; TTX, tetrodotoxin.

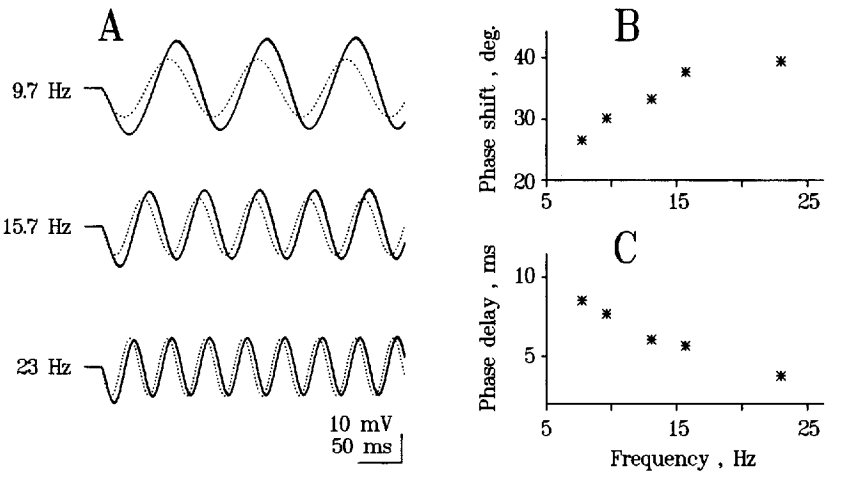

Fig. 1. Influence of modulation frequency on phase shifts of membrane potential oscillations. (A) Membrane potential oscillations (continuous lines) evoked by injection of sinusoidal currents (0.15 nA, dotted lines) at three different modulation frequencies. Membrane potential traces show the superposition of five individual responses. Note the reduction of phase delay and amplitude of the response with increasing modulation frequency. (B) Dependence of the angular phase shift of the voltage response (ordinate, degrees) on modulation frequency (abscissa, Hz). (C) Dependence of the phase delay of the voltage response (ordinate, ms) on modulation frequency (abscissa, Hz). Data in A–C are from the same cell.

the integration of synaptic input. To this end we obtained whole-cell recordings from cells in layers II/III of rat visual cortex slices, imposed periodic fluctuations of the membrane potential by current injection and examined the effect of this modulation on the timing of action potentials that were evoked either by current injection alone or in combination with synaptic activation.

EXPERIMENTAL PROCEDURES

Slices of the visual cortex of three- to six-week-old Wistar rats (Charles River GmbH, Suzfeld, Germany) were prepared by conventional methods and investigated under submerged conditions at 30°C. Perfusion medium contained (in mM) 125 NaCl, 2.5 KCl, 2 $CaCl_2$, 1 $MgCl_2$, 1.25 $NaHPO_4$, 25 $NaHCO_3$, 25 D-glucose and 0.5 L-glutamine bubbled with 95% O_2 and 5% CO_2. Patch-electrodes were filled with a K-gluconate or Cs-methanesulphonate based solution (in mM: 127 K-gluconate or Cs-methanesulphonate, 20 KCl, 2 $MgCl_2$, 2 Na_2ATP, 10 HEPES, 1 EGTA) and had a resistance of 2–6 MΩ. Whole-cell recordings from pyramidal cells in layer II/III were obtained under visual control using a Nomarski optics and infrared video microscopy.[7,43] Recordings were made in a voltage-clamp or current-clamp mode. Holding potential (in the voltage-clamp mode) or the amplitude of intracellularly injected current (in the current-clamp mode) were modulated by a sine-wave signal of variable amplitude (10–50 mV; 0.05–2 nA) and frequency (10–60 Hz). Synaptic responses were evoked by electric shocks applied through stimulation electrodes located 0.5–1.5 mm below or lateral to the recording site. Synaptic stimulation was applied at different phase angles relative to the induced oscillations of the membrane potential. After amplification (EPC-7, List Electronic or Axoclamp-2A, Axon Instruments) data were digitized at 5 or 10 kHz and fed into a computer (PC-386; Labmaster, TL-1 DMA interface and pCLAMP software, Axon Instruments) for off-line processing.

RESULTS

Relation between induced oscillations and spike timing

Whole-cell recordings were obtained under visual control[7,43] from 31 pyramidal cells in layers II–III of rat visual cortex slices. Oscillations of the membrane potential were induced by injecting sinusoidal currents through the recording pipette. The modulation of the membrane potential followed that of the injected current with a phase shift that depended on the modulation frequency (Fig. 1A). While phase angles increased with increasing frequency (Fig. 1B) the absolute value of the delay (in ms) between the peaks of injected current and resulting deflections of membrane potential decreased at higher frequencies (Fig. 1C). With frequencies of modulating current of 10–20 Hz the delay of membrane potential oscillations varied in different cells from 3 to 19 ms (average 8.4 ± 1.2 ms, n=29), reflecting the difference in membrane time constants. Membrane time constants estimated from responses to rectangular current pulses varied from 8 ms to 25.2 ms (average 18.8 ± 2.26, n=10). As expected the magnitude of the phase shift was positively correlated with the membrane time constants (data not shown). Another effect of increasing modulation frequency was a reduction of the amplitude of the cells' response (Fig. 1A). This high frequency attenuation was also more pronounced in cells with long time

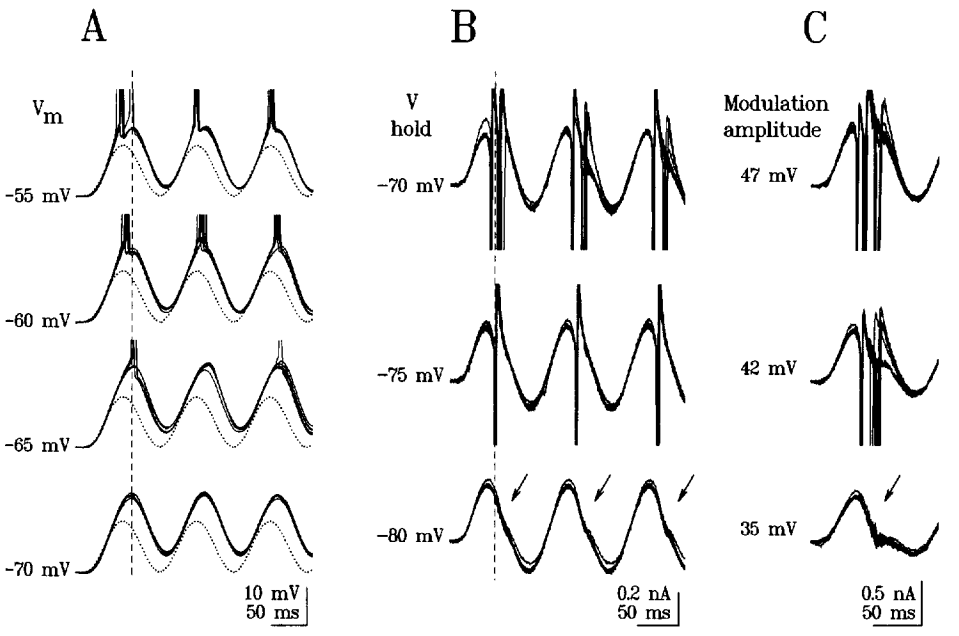

Fig. 2. Dependence of the phase lag of spike generation on membrane potential (A, current-clamp), on holding potential (B, voltage-clamp) and the modulation amplitude (C, voltage-clamp). (A) Effects of shifting the membrane potential by injecting d.c. current as indicated. The amplitude of the sinusoidal current (0.33 nA, dotted traces) was kept constant. Note that spikes occur increasingly earlier and more consistently as the membrane potential is shifted towards more positive values. (B) Effect of shifting the holding potential on spike timing in another cell recorded in voltage-clamp. The amplitude of the sinusoidal modulation of the holding potential was kept constant (38 mV). Note the subthreshold responses on the trailing slope of the oscillations at a holding potential of −80 mV (arrows), and the decreasing phase lag of suprathreshold currents at more depolarized holding potentials. (C) Effect of increasing modulation amplitude in another cell recorded in voltage-clamp. Average holding potential was −75 mV, modulation amplitude was varied as indicated. Note the instabilities on the falling slope of the response to subthreshold modulation and the phase advance of spikes with increasing modulation amplitude. Each trace contains five (A) or 10 (B,C) superimposed responses. Vertical interrupted lines in A,B show the timing of spikes at threshold. Spikes are truncated in this and the following figures.

constants indicating that it was due to the passive R-C properties of the membrane.[10,33]

In order to examine the influence of voltage-dependent conductances on the induced oscillations and to study the timing of spikes, the membrane potential was varied by adding a d.c. component to the injected current (n=6). As the depolarizing cycles came close to threshold, the membrane potential began to jitter, suggesting transient activation of voltage-gated conductances, and with further depolarization these instabilities triggered action potentials. Initially these appeared at the positive peak of the membrane potential oscillations (Fig. 2A, traces at −65 mV), and hence with a delay relative to the peak of the injected sine-wave current. With further depolarization the spikes occurred progressively earlier within the oscillation cycle reducing the phase lag between injected currents and spike generation (Fig. 2A).

In the voltage-clamp mode, the membrane potential oscillations were induced by a sine-wave modulation of the holding potential (n=20 cells). At holding potentials and modulation amplitudes that were subthreshold, noisy fluctuations occurred on the falling slopes of the current traces, indicative of activated inward currents (arrows in Fig. 2B and C, lower traces). The duration of these noisy fluctuations decreased with increasing modulation frequency. At 9.5–11 Hz (n=10) average duration was 16.6 ± 1.84 ms and at 20 Hz (n=8) it was 7.3 ± 0.76 ms. When the holding potential was shifted towards more depolarized levels, these fluctuations generated spikes whose phase lag decreased and whose number per oscillation cycle increased with increasing depolarization (Fig. 2B). Keeping the average holding potential constant but increasing the modulation amplitude had a similar effect. Subthreshold modulation activated fluctuating inward currents (arrow in Fig. 2C, bottom traces). Stronger modulation generated spikes whose phase lag relative to the injected current decreased, and whose number per cycle increased with increasing modulation amplitude (Fig. 2C). Both the subthreshold current fluctuations and spikes were reversibly blocked by bath application of tetrodotoxin (0.3 μM, n=3 cells, data not shown), suggesting that they primarily depended on activation of voltage-gated sodium conductances.

The current required to evoke spikes depended markedly on the frequency of modulation, more

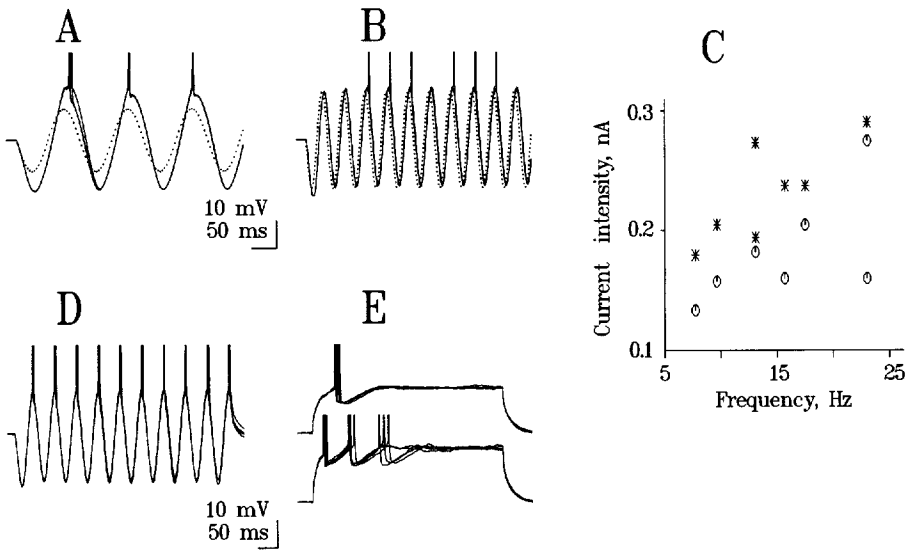

Fig. 3. Dependence of spike generation on modulation frequency. (A,B) Responses of a cell (continuous lines) to sinusoidal current (dotted lines) of different frequency and amplitude (7.8 Hz and 0.18 nA in A; 23 Hz and 0.29 nA in B). Note occurrence of discharge failures in B despite increased current amplitude. (C) Scatter plot showing the combinations of modulation frequencies (abscissa) and current intensities (ordinate) that led to spike discharges (asterisks) or failed to evoke spikes (open symbols). Note that the current required to evoke spikes increases with modulation frequency. Same cell as in A,B. (D) Responses of a cell to injection of sinusoidal current (17.5 Hz, 0.24 nA). (E) Responses of the same cell to a current step of the same amplitude (upper traces, 0.24 nA) and to a step of higher amplitude (lower traces, 0.3 nA). Note that current steps evoke less spikes with greater latency jitter than sinusoidal currents.

current being required at higher frequencies. In the cell exemplified in Fig. 3A, current with a peak amplitude of 0.18 nA was sufficient to induce action potentials at a modulation frequency of 7.8 Hz while 0.29 nA were required at 23 Hz (Fig. 3B). The scatter diagram in Fig. 3C shows that this relation holds throughout the range of examined frequencies (8–23 Hz). Repeated determination of spike threshold with injection of rectangular current pulses confirmed that this threshold remained constant (−50 mV) throughout the experiment. As suggested by the reduced amplitude of membrane potential changes at higher frequencies a likely reason for the threshold increase is the frequency dependent change of input impedance.[10,33]

Still, oscillatory currents were more effective than sustained currents in evoking multiple discharges; moreover, responses to the former exhibited less temporal jitter. As exemplified in Fig. 3D and E, oscillatory current evoked a train of precisely-timed spikes while a sustained pulse of equal amplitude (0.24 nA) elicited only a single spike whose latency varied. Increasing the amplitude of the current step to 0.3 nA led to repetitive but still less sustained discharges whereby later spikes exhibited considerable latency scatter. This response pattern was characteristic for the whole sample of regular spiking cells. Another feature of responses to sinusoidal current was a gradually increasing phase lag of the repetitive discharges. This increase in phase lag went in parallel with an increase in spike failures, an increase in the jitter of spike timing and a reduction

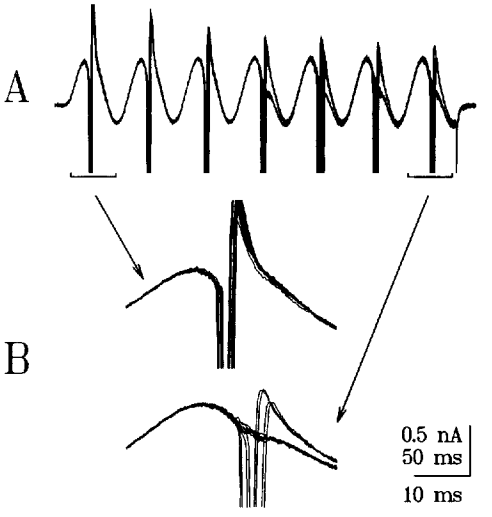

Fig. 4. Phase changes of spikes recorded in voltage-clamp mode during prolonged sinusoidal modulation of the holding potential. (A) Currents evoked by sinusoidal modulation (20 Hz, 23 mV) of the holding potential (−60 mV). 10 superimposed responses. (B) Responses to the first and seventh cycle at expanded time scale. Spikes evoked during the seventh cycle are delayed, less reliably evoked and have smaller afterhyperpolarizing potentials.

of spike associated currents. This behaviour was found in 11 of 15 cells and is exemplified in Fig. 4. In the remaining four cells (data not shown) the phase lag of spikes remained constant during six oscillation cycles but the probability of spike occurrence decreased.

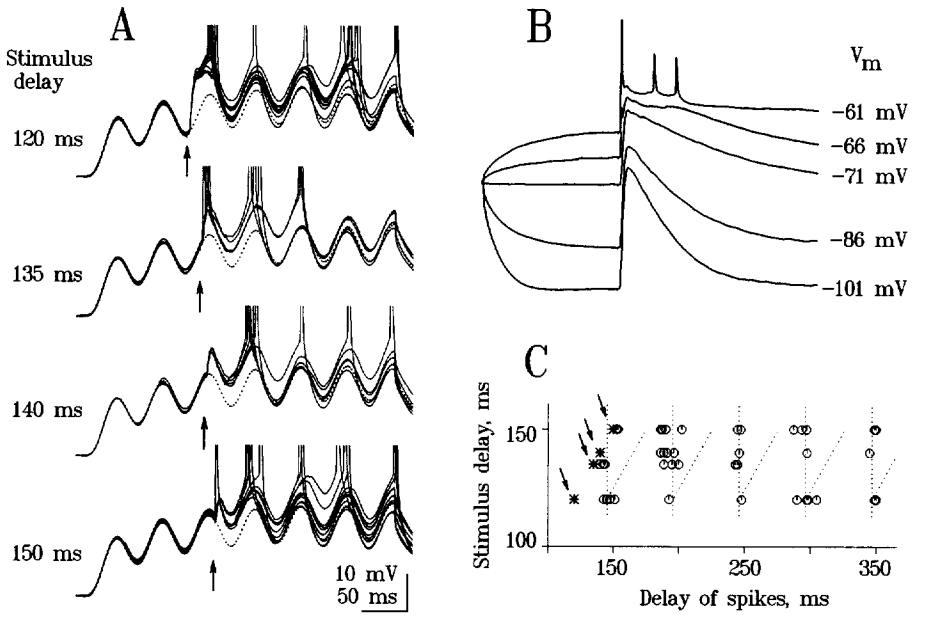

Fig. 5. Combination of subthreshold synaptic activation with oscillatory modulation of the membrane potential in a pyramidal layer II/III cell recorded in current-clamp. (A) Response to afferent stimulation applied at different delays relative to the onset of the sinusoidal modulation (20 Hz) of the membrane potential. Arrows: time of afferent stimulation. Initial membrane potential: −71 mV. Traces represent superpositions of five to 10 individual responses and one average (n=5, dotted trace) of responses evoked by the sinusoidal current alone. Note that a single stimulus gives rise to a sequence of spikes riding on the positive peaks of oscillations and that changing the delay of afferent stimulation does not cause a parallel shift in the latency of the first spike and has little effect on the timing of further discharges. (B) Responses of the same cell to afferent stimulation alone, recorded at different membrane potentials as indicated. Note a long-lasting component of the response, the amplitude of which increases with depolarization. Each trace is an average of five responses. Additional spikes in the uppermost trace are reduced in amplitude because of averaging. Calibration is common for A and B. (C) Spike delays (abscissa) plotted against delays of synaptic activation (ordinate) relative to the onset of sinusoidal modulation of the membrane potential. Data are from the same cell as in A, B. Each point represents an individual spike. Asterisks with arrows mark the time of afferent stimulation. Vertical dotted lines indicate the location of the positive peaks of the membrane potential oscillations, oblique dotted lines indicate shifts in response latency expected from linear extrapolation of stimulus delays.

Interaction between synaptic activation and induced oscillations

Excitatory postsynaptic responses (n=13) were evoked by applying electrical shocks through stimulation electrodes, positioned 0.5–1.5 mm lateral to or below the recorded neuron. These synaptic events were then paired with the imposed membrane potential oscillations whereby stimulus strength and amplitude of injected current were adjusted so that both the synaptic response and the membrane oscillations remained subthreshold when evoked in isolation.

By varying stimulation intensity we evoked either large and long-lasting (n=9) or small and short-lasting (n=4) synaptic responses. The strong synaptic responses typically had amplitudes of 10–20 mV (excitatory postsynaptic potentials, EPSPs; n=3) or 0.5–2 nA (excitatory postsynaptic currents, EPSCs; n=6) and lasted for more than 100 ms (range 120–300 ms). In four cells the long duration of the response was due to activation of *N*-methyl-D-aspartate (NMDA) receptors because the EPSP decayed more rapidly when the cells were hyperpolarized. In five cells the long duration was caused by polysynaptic input.

A typical example of an EPSP with a pronounced NMDA receptor mediated component is illustrated in Fig. 5. The long-lasting component of this response was enhanced by depolarization and suppressed by hyperpolarization indicating that it was due to activation of NMDA receptors.[30] The early component of the EPSP showed the classical voltage dependence of α-amino-3-hydroxy-5-methylisoxazole-4-propionate (AMPA) receptor-mediated responses: it increased with hyperpolarization and decreased with depolarization (Fig. 5B). When this EPSP was paired with a sufficiently strong step depolarization of the membrane potential it elicited a short latency spike that was followed on two occasions by a further spike. However, when paired with induced oscillations the same EPSP evoked a long train of discharges that occurred at the positive peaks of the membrane potential oscillations (Fig. 5A). Changing the phase angle of synaptic activation relative to the oscillation cycle

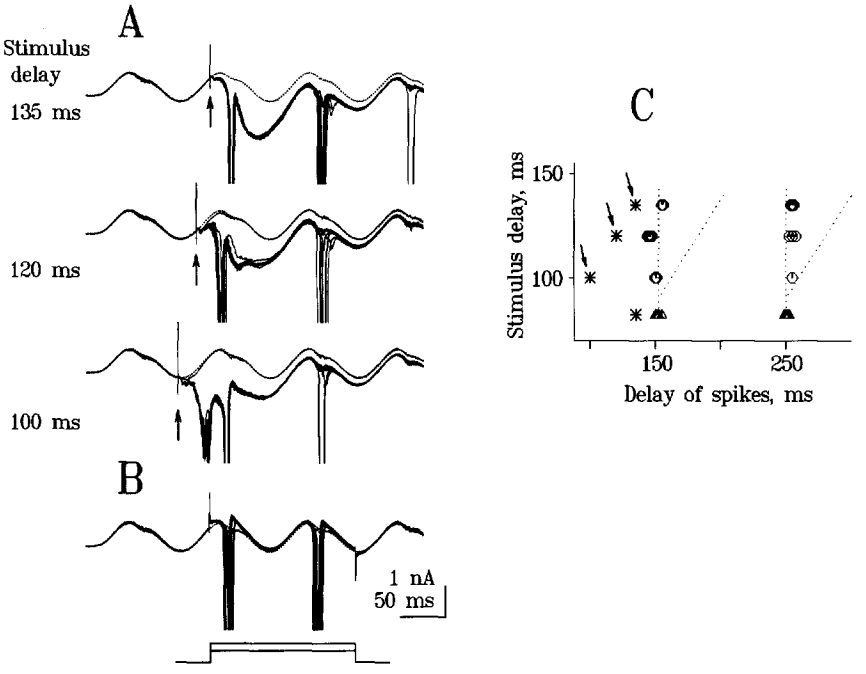

Fig. 6. Combination of subthreshold synaptic activation with oscillatory modulation of the holding potential in a cell recorded in voltage-clamp. (A) Current responses to afferent stimuli (arrows) applied at different delays relative to the onset (phase) of sine-wave modulation (10 Hz) of the holding potential. Traces show 10 superimposed individual responses and one average (n=10, dotted trace) of the response to modulation of holding potential alone. Note that a single afferent stimulus evokes two to three widely-spaced spikes which are phase locked to the oscillation cycle whereby the latency of the first spike is influenced only little and that of the second not at all by changes in stimulus delay. (B) Current responses evoked in the same cell as in A by pairing sinusoidal modulation of the holding potential with an additional voltage step (3 or 5 mV). Timing of the voltage step is indicated at the bottom. Traces show 10 superimposed responses. Note that timing of spikes relative to the oscillation cycle is similar to that of the synaptically-evoked responses. (C) Spike delays (abscissa) plotted against delays of synaptic activation (ordinate) for the cell shown in A, B. Conventions are the same as in Fig. 4C. The asterisk without arrow marks the beginning of the additional current step in B, and triangles show the timing of spikes evoked by this step.

had only little effect on the timing of the first spikes in the sequence and virtually no effect on the timing of later discharges. As indicated in Fig. 5C, the latency shift of the first spike was smaller than the objective shift in the timing of the stimulus; later spikes were completely independent of stimulus timing and strictly phase locked to the oscillation cycles (vertical dotted lines in Fig. 5C). Figure 6 demonstrates this for another cell that was recorded in the voltage-clamp mode and in which the long-lasting EPSC was due to polysynaptic activation as suggested by multiple humps in the averaged response (not shown). Again, the position of the discharge relative to the oscillation cycle shifted less (by only 8–11 ms) than expected from the absolute shift of the stimulus (15 ms) and the position of the discharges in the next cycles was entirely independent of stimulus timing (Fig. 6A, upper and middle traces). When the synaptic activation was advanced by another 20 ms relative to the oscillation cycle (Fig. 6A, bottom traces) the EPSC failed altogether to evoke the first spike but it still gave rise to two later action potentials that were again phase locked to the oscillations. In this case the peak of the EPSC preceded the first spike by 21 ms. The positions of the synaptically-evoked spikes relative to the oscillation cycle (Fig. 6A and circles in Fig. 6C) were virtually identical to those of spikes evoked by the oscillations alone when these were paired with a small additional voltage step (Fig. 6B and triangles in Fig. 6C).

These results indicate that the latency and frequency of synaptic responses in cells with oscillating membrane potential are determined to a crucial extent by the parameters of the oscillations. To further illustrate this dependency, we applied in six cells the same synaptic activation during induced oscillations of different frequencies. The example in Fig. 7 shows that increased oscillation frequency leads to a corresponding increase in the discharge frequency and to a decrease of the jitter of spike timing (Fig. 7B, C). Because the duration of the response is essentially the same for low and high frequency oscillations, the total number of spikes produced per EPSP is greater with high than with low oscillation frequencies. Although plausible, this is remarkable as not only the synaptic activation, but also the total amount of current injected in the two cases is the same.

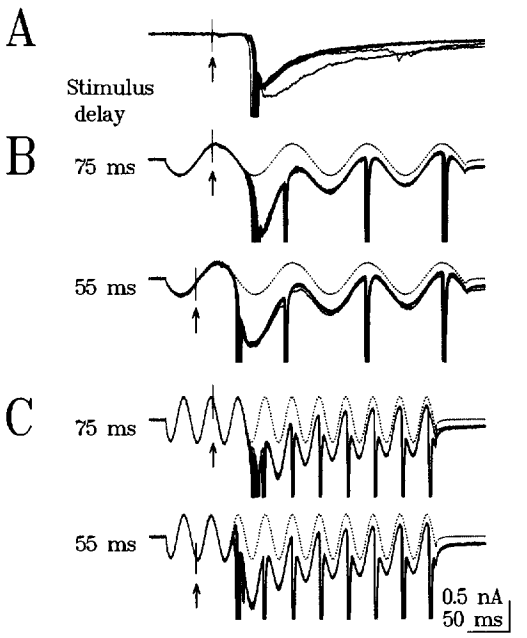

Fig. 7. Combination of synaptic activation with subthreshold oscillatory modulation of the holding potential at different frequencies. (A) Polysynaptic response to orthodromic activation (arrow) recorded in voltage-clamp mode. Superposition of 10 responses. Holding potential: −70 mV. (B,C) Current responses to the same orthodromic stimulation as in A applied at different phases (arrows) of sine-wave modulation at 10 Hz (B) and 24 Hz (C). Traces are superpositions of 10 responses and one average (n=10, dotted trace) of responses evoked by the sinusoidal current alone. Note that the temporal patterning, the frequency and the number of spikes in response to the same synaptic stimulus change markedly with oscillation frequency and do not depend on the phase angle of the stimulus relative to the oscillation cycle. Note also that the time of occurrence of the spikes subsequent to the first one is independent of stimulus timing and that the temporal jitter of spikes is reduced at higher oscillation frequency.

The finding that synaptically-evoked discharges are strictly phase locked to the oscillation cycle indicates that there is a narrow window of heightened excitability. In order to determine the gating characteristics of this window for synaptic responses, we evoked weak, short-lasting EPSCs (amplitude 30–150 pA, duration 8–25 ms) at different phases of the oscillation cycle. This revealed that the temporal window during which a weak synaptic input triggered a spike was very narrow and in the range of a few milliseconds. In the case shown in Fig. 8 spikes were generated reliably only when the stimulus was presented within a 2 ms window (Fig. 8A,B). This window corresponds precisely to the region where subthreshold modulation of the membrane potential produced instabilities (Fig. 8C, oblique arrow). Shifting the stimulus position by only 2–3 ms away from this window dramatically reduced the probability of spike generation or even completely prevented spike responses (Fig. 8A,B). Analysis of three more cells that were modulated at 10 Hz revealed window durations in the range of 4 to 7 ms. The effect of this gating was that responses to the effective stimuli were again locked to the oscillation cycle with a latency jitter much smaller than predicted from the variations in stimulus timing.

DISCUSSION

The results of this study show that passive modulation of the membrane potential with sinusoidal currents leads to periodic activation of voltage-gated conductances (predominantly sodium) and as a consequence to periodic instabilities of the membrane during which the probability of spike generation is greatly enhanced. A similar effect is expected to occur under natural conditions when oscillatory fluctuations of the membrane potential are induced either by pacemaker currents or by network interactions leading to cyclic alternation of excitatory and inhibitory inputs (see Introduction). In these natural cases of oscillatory behaviour, conditions are more complex because the membrane potential oscillations are associated in addition with cyclic changes in membrane resistance due to oscillatory synaptic input and probably also pacemaker currents. This complicates the effects which membrane potential oscillations have on the transmission of synaptic input but the basic principles of interference are likely to be the same as with passive modulation. It is even to be expected that the precision with which input activity gets selected and output activity gets patterned is higher under natural conditions because membrane time constants are shortened and active outward currents can veto transmission more effectively and promptly than the hyperpolarization induced with current injection.

Gutfreund *et al.*[10] and Hutcheon *et al.*[15] have shown that cortical neurons exhibit a frequency-dependent resonance to injection of sinusoidal currents that manifests itself by enhanced modulation of the voltage response and is due to the combined action of a hyperpolarization-activated cation current, an inwardly rectifying K^+ current and a persistent Na^+ current. We have not studied systematically the frequency response of our neurons and therefore do not know to which extent these currents contributed. The frequencies where these resonance phenomena were prominent were considerably lower (0.7–2.5 Hz) than the frequencies used in the present study as long as the modulation range was centred around the resting potential and remained subthreshold. This makes it unlikely that these resonance phenomena contributed to the excitability changes observed in the present experiments. Further experiments are required, however, to identify the nature of the tetrodotoxin (TTX)-sensitive Na^+-current evoked by our high frequency oscillations.

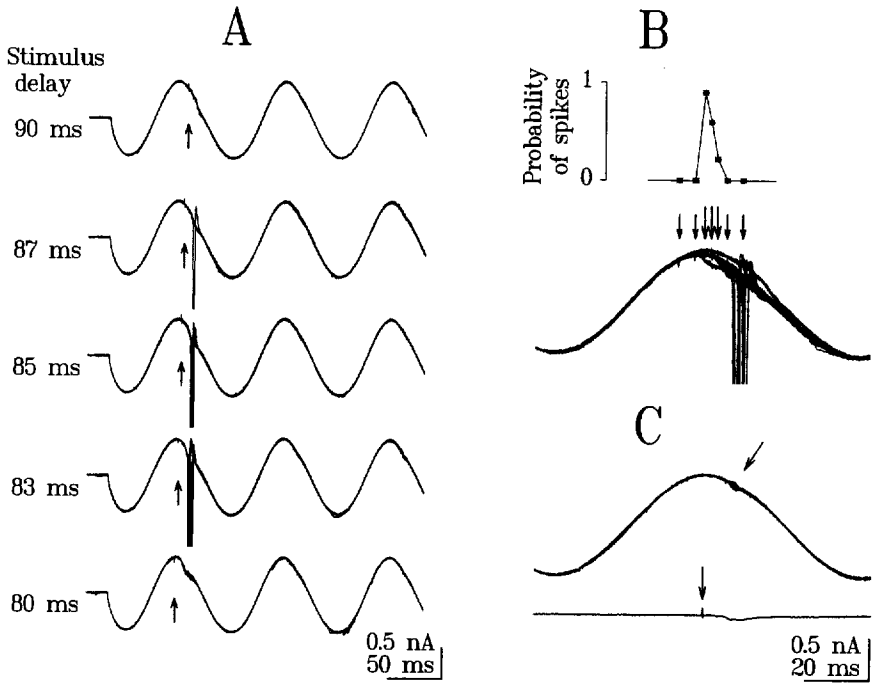

Fig. 8. The effect of oscillatory modulation of the membrane potential on responses to weak synaptic inputs. (A) Current responses evoked by combining subthreshold oscillatory modulation of the holding potential (10 Hz) with subthreshold synaptic activation applied at different phases of the oscillation cycle (arrows). Traces are superpositions of five to 10 individual responses. (B) Probability of spike generation as a function of the position of the afferent stimulus relative to the oscillation cycle. Upper graph: Probability distribution. Lower traces: Superpositions of 35 individual responses to afferent stimuli applied at times indicated by arrows. Larger arrows mark stimuli which evoked spikes. Note that spikes are triggered only when afferent stimulation is applied during a critical window of the oscillation phase that lasts about 4 ms. (C) Superposition of 10 responses to modulation of the holding potential alone (upper traces) and averaged response (n=10) to synaptic activation alone (bottom trace). Note that timing of spikes in B corresponds to the period of membrane instability in C (oblique arrow).

Temporal patterning of discharges

With respect to information processing the most influential effect of the induced oscillations is probably that slowly decaying EPSPs elicit long trains of action potentials that are locked to a particular phase of the oscillation cycle. This has three important implications. First, the timing of the output activity of a cell can become relatively independent of the time of arrival of EPSPs. Second, a single EPSP can trigger a train of regularly spaced action potentials and, third, the frequency, and hence also the total number of discharges in this sustained postsynaptic response gets determined by the frequency of the membrane potential oscillations rather than by the amplitude of the EPSP. Thus, with an oscillatory modulation of the membrane potential close to threshold, the most important variables of responses to synaptic input, their temporal structure, magnitude and to a great extent even latency, are determined predominantly by the state of the postsynaptic neuron and become partly independent of the input patterns. One effect is that responses to sustained synaptic input such as provided by NMDA receptor-mediated or polysynaptic activity undergo a precise temporal patterning. Another effect is that these responses get amplified whereby the degree of amplification depends directly on oscillation frequency. Under steady-state conditions the same EPSPs, even if paired with a steady membrane depolarization, generally induce only one or two spikes. Thus, the synaptic input assumes the function of a gate that enables the cell to fire but it is the postsynaptic cell that determines the essential characteristics of the response rather than the input. In this context it is also noteworthy that an oscillatory modulation of the membrane potential was more effective in generating long trains of spikes than a sustained depolarization of the same amplitude. Factors limiting repetitive firing are inactivation of Na^+-currents and activation of both voltage- and Ca^{2+}-gated K^+-conductances. The cyclic hyperpolarizations associated with the oscillatory modulation antagonize both processes by accelerating reactivation of Na^+-conductances and by reducing the activation of K^+-conductances. The latter is likely to result from direct effects on voltage-gated K^+-conductances and from a reduction of Ca^{2+}-entry through NMDA- and voltage-gated Ca^{2+}-channels and secondary decrease of Ca^{2+}-dependent K^+-conductances. An additional

possibility is that the cyclic depolarizations provided particularly favourable conditions for the transient activation of Na^+-conductances. This is suggested by the TTX sensitive instabilities that occurred during the depolarization cycles. Finally, it is conceivable that some components of receptor desensitization are voltage-dependent and attenuated by hyperpolarizing cycles.

Precise coincidence detection in oscillating cells

Another consequence of the oscillatory modulation of the membrane potential is a heightened sensitivity of the postsynaptic neuron to the precise timing of synaptic input. This effect is particularly pronounced for weak, short-lasting EPSPs. As the data show, such inputs can reach threshold only within a narrow temporal window, whose duration decreases with increasing modulation frequency, as indicated by the shortening of the period during which voltage-gated inward currents are activated. In cells oscillating at frequencies in the α and lower β-range this window is in the range of a few ms and thus considerably shorter than the integration interval predicted from membrane time constants under stationary conditions. Thus, cells subjected to an oscillatory modulation of the membrane potential become very sensitive to the precise timing relations of synaptic inputs.

This result is important in the context of the ongoing debate[20] about the hypothesis that synchronization of neuronal discharges is exploited in cortical processing and serves to select subsets of responses for further joint processing (binding) by selectively increasing their saliency (for review see Ref. 38). A critical prerequisite for this conjecture is that neurons can function as coincidence detectors with a temporal precision in the millisecond range and that the timing of discharges can be precisely controlled. Some authors conclude that these constraints cannot be met by cortical neurons[34] while others argue that they can.[19,20,26,32,39,45] The present data suggest that the temporal precision of input selection and output timing can be raised substantially and reach the level postulated by the synchronization hypothesis if cells get recruited into an oscillatory network. Moreover, the ability of oscillations to delay spiking in response to synaptic input until a particular phase of the oscillation cycle is reached is ideally suited to synchronize distributed responses. Together with the observation that precise synchronization is often associated with an oscillatory patterning of responses[19] this suggests that oscillations could be instrumental for the generation of precise temporal relations. A function requiring extreme precision in evaluating temporal relations is the location of sound sources by measuring interaural delays.[6] In this context it is noteworthy that a recent simulation study aimed at explaining the astounding temporal precision in auditory localization has also applied an oscillatory patterning of responses in order to increase temporal resolution and precision.[8]

Further possible functions of oscillations

The option to delay responses to synaptic input and to generate responses at a particular phase angle of the oscillation may also be exploited for functions other than synchronization. Hippocampal place cells seem to encode spatial position not only in their discharge rate but also in the phase angle of discharges relative to the ongoing theta oscillations.[31] It has also been proposed that oscillations could serve to generate temporal codes by converting amplitude differences among input signals into latency differences of output signals.[11] Our data show that such phase and latency shifts can occur and that the magnitude of the shift depends on the strength of the input signal, the time constants of the membrane, the level of the average membrane potential and the modulation depth and the frequency of oscillatory fluctuations. These variables are all subjected to dynamic modifications by both sensory input and internally generated modulatory signals. Modulatory inputs from central core structures such as the brainstem, the intralaminar thalamic nuclei and the basal forebrain change preferred oscillation frequencies over a wide range and facilitate the occurrence of γ-oscillations.[29,40–42] In addition, these projections influence voltage and Ca^{2+}-dependent K^+-conductances and thereby modify resting membrane potential levels and effective membrane time constants (for review see Ref. 42). Altogether this provides a rich repertoire of options to influence the temporal relations between synaptic input and postsynaptic responses and to form assemblies of synchronously firing cells that are either active at different cycles or phase angles of a common oscillatory pattern or that oscillate at different frequencies. Notably, changes of membrane time constants, or average membrane potential or modulation depth will only shift the phase angle of responses while preserving the overall temporal patterning, a wanted property of neuronal networks that exploit precise timing for information processing. However, our data also show that for a given oscillatory patterning the phase angle of the responses depends only little on the amplitude of the synaptic drive, especially at higher oscillation frequencies, because of the short duration of transient inward currents. Responses to the long lasting EPSPs occurred with precisely the same phase angle throughout the decay phase of the EPSP. Changing the amplitude of such slowly decaying EPSPs is thus unlikely to produce a systematic phase shift of the whole spiking pattern. However, because the phase angle of the transient sodium conductance depends on the modulation depth and the d.c.-offset of the oscillations, control of these parameters could be used very effectively to produce

systematic phase shifts among the firing patterns of neurons, as proposed by Hopfield.[11]

In order to obtain a more realistic appreciation of the temporal integration properties of the neurons engaged in oscillatory activity, it is indispensable, however, to study input–output functions in neurons that are actually part of an oscillating network. The expectancy is that the periodic fluctuations of membrane resistance caused by oscillatory input from inhibitory neurons together with periodically-activated voltage-gated conductances introduces nonlinearities that sharpen the temporal filter properties of neurons well beyond the level attained in the present study with passive modulation of the membrane potential. Since it has been recently possible to induce oscillatory activity in slices of the hippocampus and neocortex that closely resembles that observed *in vivo*,[12–14,17,44,48] this goal is now within reach.

CONCLUSIONS

The present data show that generating oscillatory fluctuations of the membrane potential is a powerful strategy to establish temporally-structured activity patterns, to synchronize discharges of interconnected neurons and to establish precise temporal relations between the discharges of simultaneously active cells. On the one hand, it allows delay of the output of a neuron until a particular phase of the oscillation cycle is reached, on the other hand, it permits specification of narrow temporal windows for the integration and propagation of the activity with the effect that only inputs which are active during these windows will summate effectively and be relayed further. Thus, the networks engaged in oscillatory activity become much more sensitive to the precise timing of signals than one would expect from the time constants that characterize synaptic integration under steady-state conditions.

Acknowledgements—We are grateful to Mrs Christa Schlauss for the excellent technical assistance and to Prof. Ulf Eysel for the generous support of this project at its final stage. This project was partially supported by the Max-Planck Society and Deutsche Forschungsgemeinschaft Ey 8/23 and SFB 509/TP A5.

REFERENCES

1. Alonso A. and Llinas R. (1989) Subthreshold Na^+-dependent theta-like rhythmicity in stellate cells of entorhinal cortex layer II. *Nature* **342,** 175–178.
2. Alonso J.-M., Usrey W. M. and Reid R. C. (1996) Precisely correlated firing in cells of the lateral geniculate nucleus. *Nature* **383,** 815–819.
3. Bragin A., Jando G., Nadasdy Z., Hetke J., Wise K. and Buzsaki G. (1995) Gamma (40–100 Hz) oscillation in the hippocampus of the behaving rat. *J. Neurosci.* **15,** 47–60.
4. Buhl E. H., Cobb S. R., Halasy Y. K. and Somogyi P. (1995) Properties of unitary IPSPs evoked by anatomically identified basket cells in the rat hippocampus. *Eur. J. Neurosci.* **7,** 1987–2004.
5. Cobb S. R., Buhl E. H., Halasy K., Paulsen O. and Somogyi P. (1995) Synchronization of neuronal activity in hippocampus by individual GABAergic interneurones. *Nature* **378,** 75–78.
6. Dear S. P., Simmons J. A. and Fritz J. (1993) A possible neuronal basis for representation of acoustic scenes in auditory cortex of the big brown bat. *Nature* **364,** 620–623.
7. Dodt H.-U., Zieglgänsberger W. (1990) Visualizing unstained neurones in living brain slices by infrared DIC-videomicroscopy. *Brain Res.* **537,** 333–336.
8. Gerstner W., Kempter R., van Hemmen L. J. and Wagner H. (1996) A neuronal learning rule for sub-millisecond temporal coding. *Nature* **383,** 76–78.
9. Gray C. M. and McCormick D. A. (1996) Chattering cells: superficial pyramidal neurones contributing to the generation of synchronous oscillations in the visual cortex. *Science* **274,** 109–113.
10. Gutfreund Y., Yarom Y. and Segev I. (1995) Subthreshold oscillations and resonant frequency in guinea-pig cortical neurones: physiology and modelling. *J. Physiol., Lond.* **4833,** 621–640.
11. Hopfield J. J. (1995) Pattern recognition computation using action potential timing for stimulus representation. *Nature* **376,** 33–36.
12. Huerta P. T. and Lisman J. E. (1993) Heightened synaptic plasticity of hippocampal CA1 neurones during a cholinergically induced rhythmic state. *Nature* **364,** 729–735.
13. Huerta P. T. and Lisman J. E. (1995) Bidirectional synaptic plasticity induced by a single burst during cholinergic theta oscillation in CA1 *in vitro*. *Neuron* **15,** 1053–1063.
14. Huerta P. T. and Lisman J. E. (1996) Low-frequency stimulation at the troughs of Θ-oscillation induces long-term depression of previously potentiated CA1 synapses. *J. Neurophysiol.* **75,** 877–884.
15. Hutcheon B., Miura R. M. and Puil E. (1996) Subthreshold membrane resonance in neocortical neurons. *J. Neurophysiol.* **76,** 683–697.
16. Jahnsen H. and Karnup S. (1994) A spectral analysis of the integration of artificial synaptic potentials in mammalian central neurones. *Brain Res.* **666,** 9–20.
17. Jefferys J. G. R., Traub R. D. and Whittington A. (1996) Neuronal networks for induced 40 Hz rhythms. *Trends Neurosci.* **19,** 202–208.
18. Klink R. and Alonso A. (1993) Ionic mechanisms for the subthreshold oscillations and differential electroresponsiveness of medial entorhinal cortex layer II neurones. *J. Neurophysiol.* **70,** 144–157.
19. König P., Engel A. K., Roelfsema P. R. and Singer W. (1995) How precise is neuronal synchronization? *Neural Computat.* **7,** 469–485.
20. König P., Engel A. K. and Singer W. (1996) Integrator or coincidence detector? The role of the cortical neurone revisited. *Trends Neurosci.* **19,** 130–137.

21. Llinas R. R. (1988) The intrinsic electrophysiological properties of mammalian neurones: insights into central nervous system function. *Science* **242,** 1654–1664.
22. Llinas R., Grace A. and Yarom Y. (1991) *In vitro* neurones in mammalian cortical layer 4 exhibit intrinsic oscillatory activity in the 10 to 50-Hz frequency range. *Proc. natn. Acad. Sci. U.S.A.* **88,** 897–901.
23. Lumer E. D., Edelman G. M. and Tononi G. (1997) Neural dynamics in a model of the thalamocortical system. I. Layers, loops and the emergence of fast synchronous rhythms. *Cerebr. Cortex* **7,** 207–227.
24. Lumer E. D., Edelman G. M. and Tononi G. (1997) Neural dynamics in a model of the thalamocortical system. II. The role of neural synchrony tested through perturbations of spike timing. *Cerebr. Cortex* **7,** 228–236.
25. Lytton W. W. and Sejnowski T. J. (1991) Simulations of cortical pyramidal neurones synchronized by inhibitory interneurones. *J. Neurophysiol.* **66,** 1059–1079.
26. Mainen Z. F. and Sejnowski T. J. (1995) Reliability of spike timing in neocortical neurones. *Science* **268,** 1503–1506.
27. Markram H. and Tsodyks M. (1996) Redistribution of synaptic efficacy between neocortical pyramidal neurones. *Nature* **382,** 807–810.
28. Markram H., Lübke J., Frotscher M. and Sakmann B. (1997) Regulation of synaptic efficacy by coincidence of postsynaptic APs and EPSPs. *Science* **275,** 213–215.
29. Munk M., Roelfsema P., König P., Engel A. and Singer W. (1996) Role of reticular activation in the modulation of intracortical synchronization. *Science* **272,** 271–274.
30. Nowak L., Bregestovski P., Ascher P., Herbert A. and Prochiantz A. (1984) Magnesium gates glutamate-activated channels in mouse central neurones. *Nature* **307,** 462–465.
31. O'Keefe J. and Burgess N. (1996) Geometrical determinants of the place fields of hippocampal neurons. *Nature* **381,** 425–428.
32. Plenz D. and Aersten A. (1996) Neural dynamics in cortex-striatum co-cultures. 2 Spatiotemporal characteristics of neuronal activity. *Neuroscience* **70,** 861–891.
33. Puil E., Gimbarzevsky B. and Miura R. M. (1986) Quantification of membrane properties of trigeminal root ganglion neurons in guinea pigs. *J. Neurophysiol.* **55,** 995–1016.
34. Shadlen M. N. and Newsome W. T. (1994) Noise neural codes and cortical organization. *Curr. Opin. Neurobiol.* **4,** 569–579.
35. Silva L. R., Amitai Y. and Connors B. W. (1991) Intrinsic oscillations of neocortex generated by layer 5 pyramidal cells. *Science* **251,** 432–435.
36. Singer W. (1990) Search for coherence: a basic principle of cortical self-organization. *Concepts Neurosci.* **1,** 1–26.
37. Singer W. (1993) Synchronization of cortical activity and its putative role in information processing and learning. *A. Rev. Physiol.* **55,** 349–374.
38. Singer W. and Gray C. M. (1995) Visual feature integration and the temporal correlation hypothesis. *A. Rev. Neurosci.* **18,** 555–586.
39. Softky W. R. (1995) Simple codes versus efficient codes. *Curr. Opin. Neurobiol.* **5,** 239–247.
40. Steriade M. (1996) Awakening the brain. *Nature* **383,** 24–25.
41. Steriade M., Amzica F. and Contreras D. (1996) Synchronization of fast (30–40 Hz) spontaneous cortical rhythms during brain activation. *J. Neurosci.* **16,** 392–417.
42. Steriade M., McCormick D. A. and Sejnowski T. J. (1993) Thalamocortical oscillations in the sleeping and aroused brain. *Science* **262,** 679–685.
43. Stuart G. J., Dodt H. U. and Sakmann B. (1993) Patch-clamp recordings from the soma and dendrites of neurones in brain slices using infrared video microscopy. *Pflugers Arch.* **423,** 511–518.
44. Traub R. D., Whittington M. A., Stanford I. M. and Jefferys J. G. R. (1996) A mechanism for generation of long-range synchronous fast oscillations in the cortex. *Nature* **383,** 621–624.
45. Vaadia E., Haalman I., Abeles M., Bergman H., Prut Y., Slovin H. and Aersten A. (1995) Dynamics of neuronal interactions in monkey cortex in relation to behavioural events. *Nature* **373,** 515–518.
46. Volgushev M., Chistiakova M. and Singer W. (1995) Interaction between synaptic activation and induced membrane potential oscillations in neurones of the visual cortex. *Eur. J. Neurosci.* **8,** 77.
47. von der Malsburg C. (1981) The correlation theory of brain function. Internal report. Max-Planck-Institute for Biophysical Chemistry, Göttingen, West Germany.
48. Whittington M. A., Traub R. D. and Jefferys I. J. R. (1995) Synchronized oscillations in interneurone networks driven by metabotropic glutamate receptor activation. *Nature* **373,** 612–615.
49. Ylinen A., Bragin A., Nadasdy Z., Jando G., Szabo I., Sik A. and Buzsaki G. (1995) Sharp wave-associated high-frequency oscillation (200 Hz) in the intact hippocampus: Network and intracellular mechanisms. *J. Neurosci.* **15,** 30–46.

(*Accepted* 15 *July* 1997)